Cryogenic thermo-physical properties of additive manufactured materials

IOP Conf. Series: Materials Science and Engineering **1302** (2024) 012005 doi:10.1088/1757-899X/1302/1/012005

Cryogenic thermo-physical properties of additive manufactured materials

Klaus-Peter Weiss, Nadezda Bagrets, and Camelia Schulz

Karlsruhe Institute of Technology, Institute for Technical Physics, Hermann von Helmholtz Platz 1, 76344 Eggenstein-Leopoldshafen, Germany

E-mail: klaus.weiss@kit.edu

Abstract. Environmentally friendly aviation is one of the great challenges of this century. One promising approach is electric flight, in which an energy carrier (e.g. liquid Hydrogen LH2) and an electric powertrain work together. Within the scope of the joint project AdHyBau, the overarching goal is the development of new additive processes and fibre composite-metal hybrid designs for use in the cryogenic environment of such an electric propulsion system. Additive manufacturing of complex components for use in the cryogenic temperature range down to 20K (LH2) is one essential component in the production. For the design and optimization of the different components it is necessary to know the thermo-physical behaviour of such materials like high purity copper, Ti6Al4V alloy, Al-Mg-Sc alloy, and Inconell 718. The thermo-physical parameters investigated are thermal expansion, thermal & electrical conductivity and heat capacity. Further production-related influences coming from the method used (SLM, DED or Cold-Spray) and orientational dependences are discussed.

Supported by the Federal Ministry for Economic Affairs and Climate Action of the Federal Republic of Germany. Grant-No.: 20M1904D.

1. Introduction

The use of advanced manufacturing technologies expands the design space of lightweight components for aerospace systems and enables innovative possibilities for complex structures [1, 2]. The overall goal of the AdHyBau (*Additive Hybride Bauweisen*) joint project is to develop new additive processes and fiber composite-metal hybrid structures for use in the cryogenic environment of an aerospace electric powertrain using LH_2 (liquid hydrogen) for cooling within the system and for power generation by a fuel cell. Another goal of the project is to create end-to-end design and simulation processes to replicate reality as accurately as possible in a digital twin.

Table 1. Electric propulsion engine parameters

Total mass	50 kg
Nominal power	500 kW
Maximum torque	2000 Nm
Maximum speed	3000 rpm

The project deals with the generation of basic knowledge in order to apply innovative materials and processes in the low-temperature range and thus to examine a novel type of design of electrical

machines. The general design and simulation of the powertrain within a digital twin is carried out by Siemens AG [3, 4], components of the electric motor are investigated by Siemens AG together with the Institute of Lightweight and Plastic Engineering TU Dresden [5, 6]. The basic parameters of the 10 kW/kg electric propulsion engine are listed in Table 1. The hydrogen system of storage, distribution and utilization is developed and optimized by MT-Aerospace AG [7, 8]. Material investigations are performed at KIT together with the Fraunhofer Institute of Material Engineering [9, 10].

In Figure 1 shows the general conceptual schematic along with examples of the additively manufactured components such as heat-exchanger (HX), the motor's rotator/torque transducer and one element of internally cooled coil. Liquid hydrogen is extracted from a tank, passed through the electric motor for cooling, and redirected through a first heat exchanger (HX1) either to the tank for pressure build up or partially to a fuel cell for power generation. The re-cooled hydrogen from the line through the storage tank is also routed to the fuel cell via a second heat exchanger (HX2). Details can be found in [7].

KIT is specifically concerned with the methods for determining thermo-physical material properties and preparing the data for use in a digital twin to perform virtual tests. In this work, the characterized material properties coming from additive manufacturing, e.g. cold gas spraying (CS), selective laser melting (SLM), and direct energy deposition (DED), are reported and will be implemented in the simulation process to ensure a realistic approach.

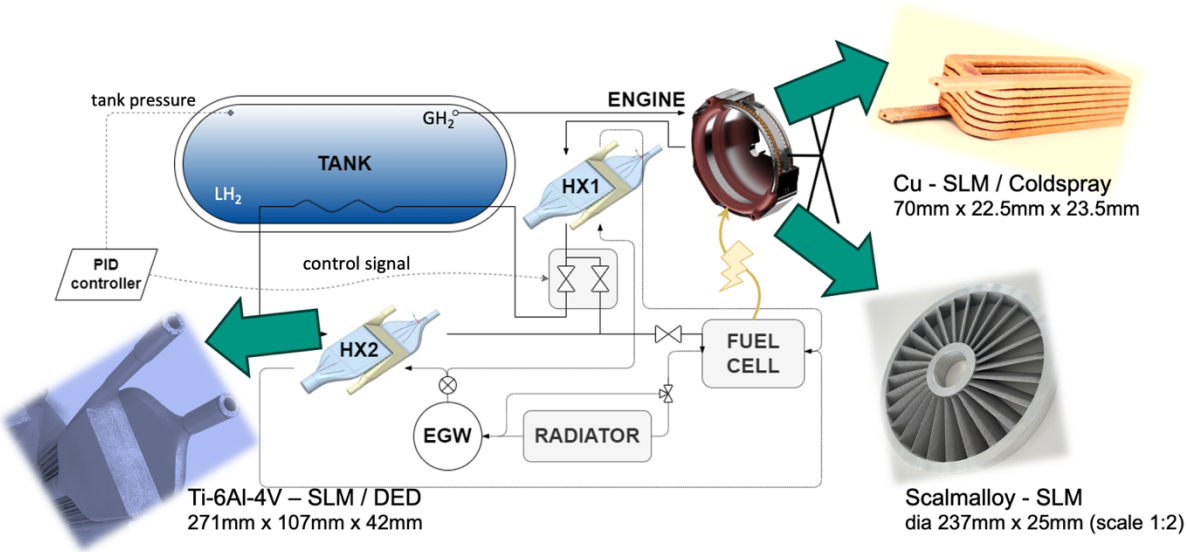

Figure 1. Conceptual scheme of the propulsion system and examples of additive manufactured components operated down to temperatures of 20 K, details can be found in [7].

2. Materials

For this cryogenic temperature range, design-relevant material properties and material models are rarely or not available. Therefore, materials for the critical structures are characterized and analyzed at KIT. This is the indispensable basis for the development of corresponding material models. The qualification methods serve as a basis for future standardization tests for successful certification for electric drives.

Materials of interest to build relevant structures are pure copper for the internally cooled motor coils, allowing optimized structures, e.g. regarding filling factor or AC losses [2, 3]. Further lightweight structures made from Scalmalloy®, specially designed Al-Mg-Sc-Zr-Mn alloy for aviation applications, for the rotator/Torque transmitter, and Ti-6Al-4V alloy for the heat exchanger [1, 7]. As structural material Inconel 718 was investigated for possible use. The materials were fabricated by the project partners using different methods as cold gas spraying (CS), selective laser melting (SLM), and direct energy deposition (DED). Although the manufacturing details are proprietary and can be found partly in [7-11], the microstructure of the investigated materials is provided to allow discussion of the results. The orientation scheme used for further discussion in this work is shown in Figure 2, far left. Here, the building direction is in z-orientation, while the deposition plane is in xy-orientation.

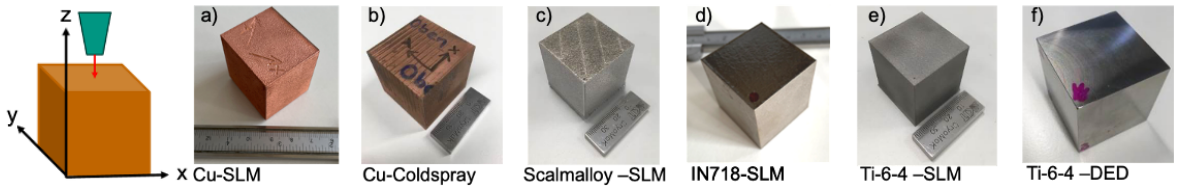

Figure 2. Additive manufactured cube material (approx. 40x40x40 mm^3) as indicated pure copper by SLM (a) and CS (b), Al-alloy Scalmalloy (c), Inconel 718 (d), Ti-6Al-4V by SLM (e) and additionally Ti-6Al-4V by DED (f).

Characterization of the thermo-physical properties are concentrated to the building z-direction or to the xy-orientation (x- and y- direction supposed to be comparable due to cross-linked build pattern in xy-plane).

While several specimen were fabricated by this method to allow mechanical tensile, fatigue or fracture tests at the Fraunhofer Institute, dedicated material cubes were provided to extract specimen for the thermo-physical measurements at KIT. The size is about 40 x 40 x40 mm^3 to allow sufficient specimen dimensions in the orientation of interest. Cubes of the different materials are shown in Figure 2 prior to specimen extraction by EDM (*electron discharge machining*).

For the coil high purity copper is used (99.999%) to achieve conductivity values as high as possible. However, the production method has a significant impact on the microstructure of the end product. In Figure 3 a-d SEM-BSE pictures are shown of the as-received material cube made by CS method taken looking in z-direction or in xy-direction. A very fine-grained structure (<10µm), twin boundaries (plastic deformation of material during coating) as well as cracks are visible due to the impact during the high energy deposition of the powder. Looking at the copper material cube coming from the SLM method by SEM-BSE in Figure 3 e-f, again in z-direction or in xy-direction, much larger grain structure is visible and less distortion.

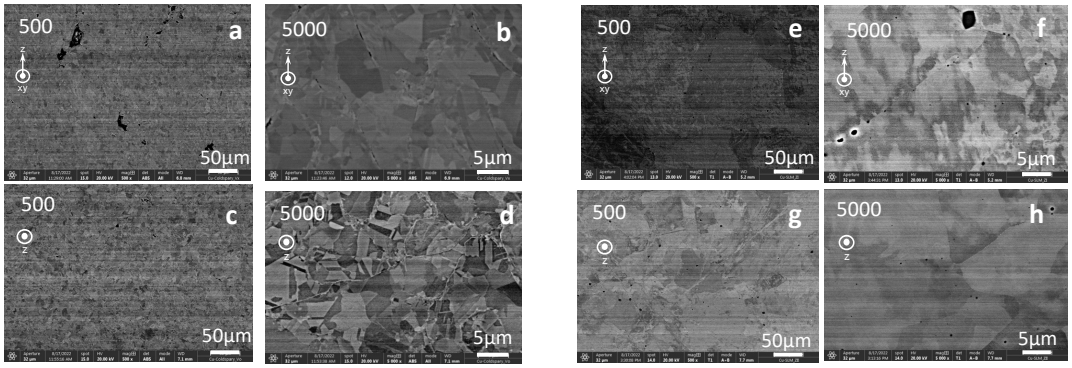

Figure 3. SEM-BSE images of Cu coldspray view in xy-direction (a & b) in z-direction (c & d), SEM-BSE images of Cu SLM view in xy-direction (e & f) in z-direction (g & h)

Scalmalloy® fabricated by the SLM method has the expected composition according to literature (see Table 2) and the micrograph is shown for the z-direction and xy-direction in Figure 4. Due to the fast solidifying a very fine-grained structure is visible in z-direction. Looking in the xy-direction the development of filament columns and larger grains in z-direction are apparent typical for such material process.

Table 2. Scalmalloy ® chemical composition (wt %)

Al balanced	Mg	Sc	Zr	Mn	Si	Fe	Zn	Cu	Ti	V	O
Min	4.0	0.6	0.2	0.3	0	0	0	0	0	0	0
Max	4.9	0.8	0.5	0.8	0.4	0.4	0.25	0.1	0.15	0.05	0.05

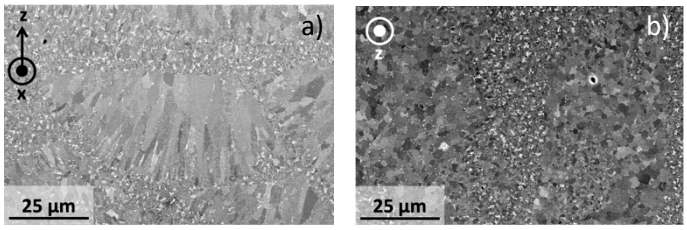

Figure 4. Micrographs of Scalmalloy® SLM view in xy-direction (a) and z-direction (b).

For lightweight components, beside of Al-alloys also Ti-alloys are feasible. Especially Ti-6Al-4V is an established composition with favourable mechanical as well as thermo-physical properties. Therefore, material from SLM as well as DED was examined and compared. The chemical composition of the used Ti-6Al-4V Grade 23 ELI (original powder and after build) is summarized for SLM in Table 3 and for DED in Table 4. After build a heat treatment for stress-relief at 650°C for 4h was performed. Differences of the manufacturing process are very clearly visible in the micrographs looking in the xy-orientation in Figure 5. While the SLM results in a very fine grain structure, the DED exhibits the typical weld like topology, again with pronounced filament columns of the grains in z-direction.

Table 3. Ti-6Al-4V for SLM powder and after build (wt %)

Ti balanced	Al	V	O	Fe	H	N
Powder	6.3	3.97	0.085	0.14	0.002	0.014
As-build	6.3	3.95	0.105	0.15	0.003	0.040

Table 4. Ti-6Al-4V for DED powder and after build (wt %)

Ti balanced	Al	V	O	Fe	H	N
Powder	6.39	3.96	0.09	0.2	0.001	0.01
As-build	6.46	3.85	0.076	0.18	0.001	0.01

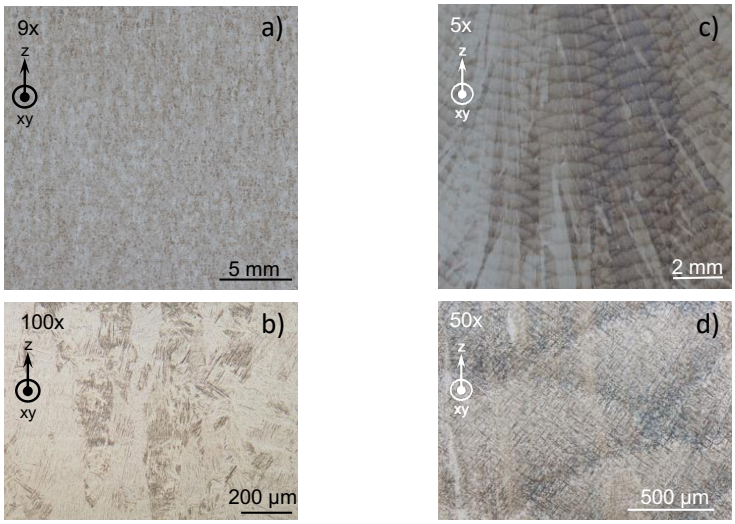

Figure 5. Micrographs of SLM (left a, b) and DED (right c, d) Ti-6Al-4V looking in xy-orientation (by courtesy of project partner MT-Aerospace).

As mentioned above Inconel 718, a precipitation hardening nickel-based alloy, as structural material fabricated by the SLM method was also characterized. The typical chemical composition is shown in Table 5. The material was annealed for solution treatment at 980 °C for 1h following a two-step

hardening annealing at 720°C for 8h cooled down with 55°C/h to 620°C staying for 8h at this temperature.

Table 5. Inconel 718 chemical composition (wt %)

Fe balanced	Ni	Cr	Mo	Nb	Mn	Ti	Al	Co	Cu	C
Min	50.0	17.0	2.8	4.75	0.00	0.65	0.2	0.0	0.0	0.00
Max	55.0	21.0	3.3	5.50	0.35	1.15	0.8	1.0	0.3	0.08

3. Experimental methods

Questions on material properties from room temperature down to cryogenic temperatures at 4.2 K are addressed in a dedicated research facility CryoMaK. The characterization possibilities range from analysis of chemical composition of alloys and microstructure to mechanical behavior (static/cyclic), as well as measurements of thermo-physical properties (expansion, heat capacity, electrical/thermal conductivity, magnetization) [12-17]. For this purpose, measurements are performed using the PPMS (*Physical Properties Measurement System*) from Quantum Design [18]. This device allows to measure the aforementioned thermo-physical properties using specific probes as shown in Figure 6. After calibration using well known standard material like nickel or copper, e.g. reported by NIST and the copper institute [19, 20], measurements were conducted in the range from about 4 K up to 300 K and partly 400 K. For high thermal and electrical conductivity, a specimen size of about 1 mm^2 cross sectional area and a measurement length in the range of 10 mm was used. A four-probe arrangement was chosen to obtain a suitable signal to noise ratio and avoid errors of heat or current flow via the sensor connection. The uncertainty of the values is less than 1%, for the thermal conductivity this value increases above 200 K due to the emissivity and radiation loss to about 2%. Heat capacity measurements were performed on a cube with the mass adjusted between 40 mg up to 100 mg depending on material density to allow a sufficient signal with the available heat pulse. The estimated uncertainty is in a range of 0.5%. The dilatometer measurement length needed to be 2 mm (+/- 0.02 mm) having a uncertainty of about 30 ppm. Measurements were conducted using slow temperature changes 0.2 K/min and below together with long settling times (0.5h to 1h) where appropriate to reach a thermally stable condition.

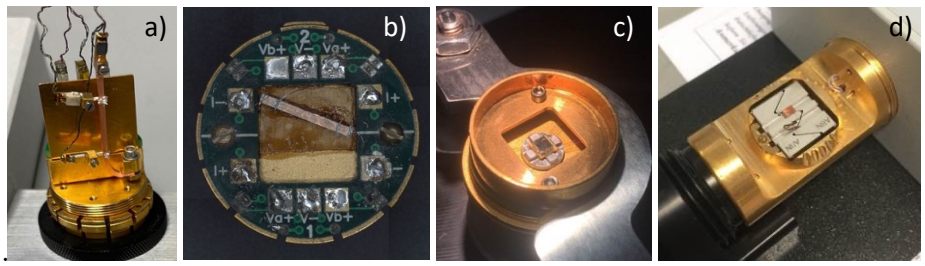

Figure 6. Used measurement probes to determine the thermal conductivity (a), electrical conductivity (b), heat capacity (c) and thermal expansion (d) within the Physical Property Measurement System of Quantum Design [18] (here shown for Cu material).

4. Experimental results

In the following, the measurement results of the investigated materials are reported. For the transport measurements Scalmalloy®, Ti-6Al-4V and Inconel 718 are shown in sections 4.1 and 4.2. The transport measurements for copper are discussed and compared separately to the end of this chapter 4 in sections 4.5 and 4.6, as a dedicated optimization of the material was performed to increase the conductivity. For the non-transport properties like thermal expansion and heat capacity, all materials are summarized in sections 4.3 and 4.4, respectively.

4.1. Thermal conductivity

Measurements were conducted as described above. Results from Scalmalloy® (SLM), Inconel 718 (SLM) and the two different Ti-6Al-4V materials (SLM and DED) exhibit no significant difference in

the z- or xy-direction (see Figure 7) and a good thermal interconnection can be obtained. As expected, the highest thermal conductivity is visible for Scalmalloy® about ten times higher than for Inconel 718 or the Ti-6Al-4V. The obtained results follow the literature data of bulk samples [19, 21, 22].

4.2. Electrical conductivity

The electric transport measurements shown in Figure 8 exhibit almost the same behavior as the thermal transport measurement. Again, the conductivity is about ten times higher for the Scalmalloy® than for Inconel 718 or Ti-6Al-4V. However, in this case a slight sensitivity to the z- or x-direction is apparent. In this case only for Inconel 718 data from bulk material was available and within the range of the obtained results [19]. For Ti-6Al-4V a superconducting transition below 5 K as reported in literature can be seen [22].

4.3. Thermal expansion

Beside of the transport measurements the quasi-static property of the thermal expansion is investigated for all materials and shown in Figure 9. A slight split of the z- and x-directions are visible. Comparing to available literature data of bulk to the additive manufactured material investigated in this work are in good agreement [19, 23, 24].

4.4. Heat capacity

No differentiation of the building directions regarding SLM, CS or DED can be examined with the heat capacity, as this property is a bulk property without direction. In Figure 10 the results of the measurement are summarized. Again, the results follow available literature data for Inconel 718, Ti-6Al-4V, and copper [24, 25, 26].

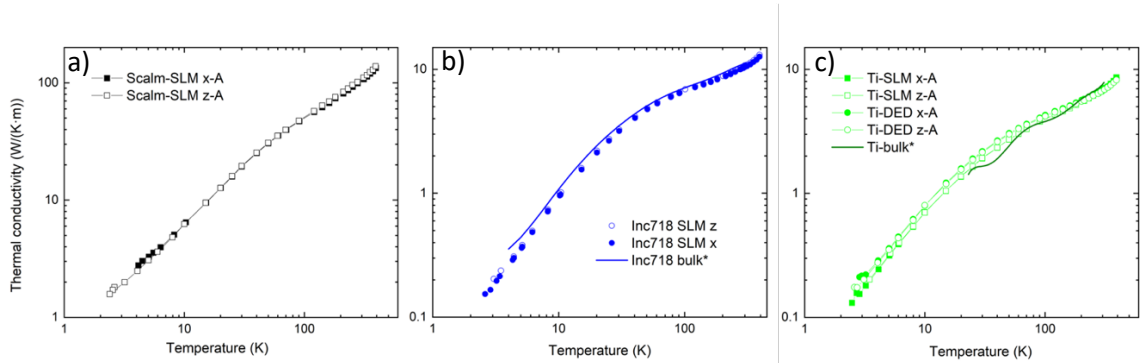

Figure 7. Thermal conductivity measurements in z- and x-direction of Scalmalloy® (SLM) (a), Inconel 718 (SLM) (b), and Ti-6Al-4V (SLM & DED) (c). As well as data of bulk material for Inconel 718[19] and Ti-6Al-4V[19] to compare.

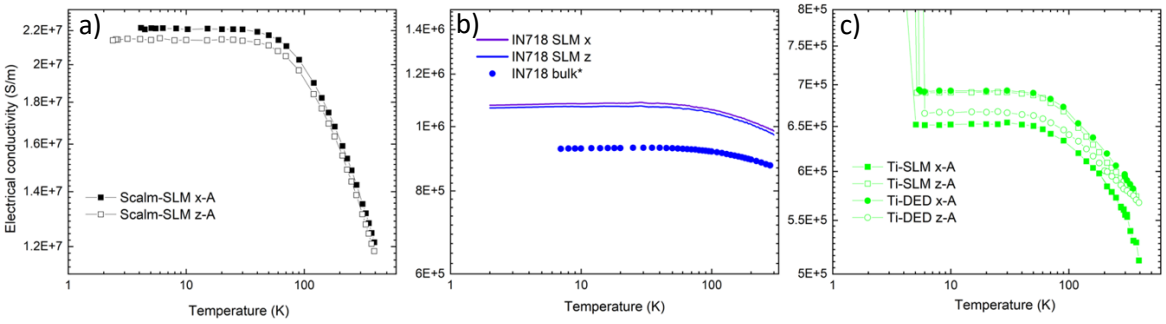

Figure 8. Electrical conductivity measurements in z- and x-direction of Scalmalloy® (SLM) (a), Inconel 718 (SLM) (b), and Ti-6Al-4V (SLM & DED) (c). As well as data of bulk material for Inconel 718[19] to compare.

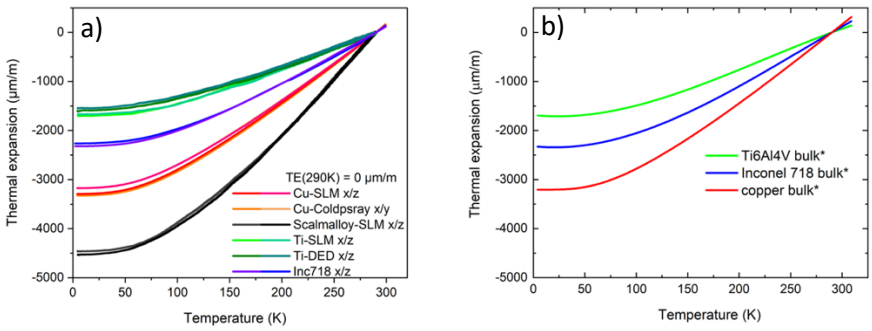

Figure 9. Thermal expansion measurement of all materials Cu (SLM, CS), Scalmalloy® (SLM), Ti-6Al-4V (SLM, DED), and Inconel 718 (SLM) in z- and x-direction (a). On the right-side literature data for comparison [19] (b).

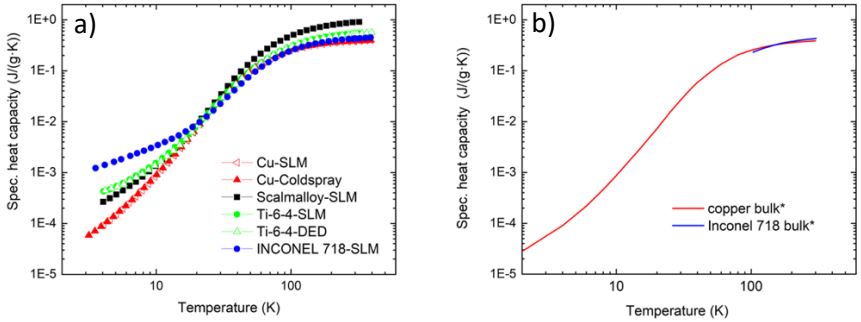

Figure 10. Heat capacity measurement of all materials Cu (SLM, CS), Scalmalloy® (SLM), Ti-6Al-4V (SLM, DED), and Inconel 718 (SLM) in z- and x-direction (a). On the right-side literature data for comparison for copper[24] and Inconel 718 [26] (b).

4.5. Cu-SLM comparison

Pure copper material was fabricated by a so-called optimized SLM process, defined by using a specific heat treatment of the obtained copper cube during fabrication to increase the thermal and electrical conductivity. Since the heat treatment was not enclosed by the supplier, a non-optimized process was requested to obtain a material condition as build and to allow a subsequent controlled heat treatment. The results of these two material characterizations are shown in Figure 11. On the left side the optimized process and on the right side the as build or non-optimized. A characteristic parameter to compare pure copper material is the *RRR*-value (*Residual Resistance Ratio*), calculated from the resistivity ratio taken at 273 K and taken at 5 K. For the optimized process a *RRR* of about 170 was obtained and the as-received approximately only half of this value of about 80. Comparing these *RRR* values with literature data the thermal and electrical conductivity are well in line with the bulk values of the related *RRR* value [20]. This allows the conclusion that the SLM process introduces distortions (e.g. grain boundaries, cracks) that lead to a reduced transportation mechanism visible in electrical and thermal conductivity. For both conditions no difference of the measurement in z- or x-direction is visible. Interestingly applying a H_V (*Vickers hardness*) test the values differ slightly with an increased hardness of the indentation in z direction compared to the xy-direction (taken from 5 measurements in each direction), as can be seen in Table 6. This can be correlated with the grain structure seen in Figure 3 of the SLM material different for the z- (fine) or the xy-direction (large).

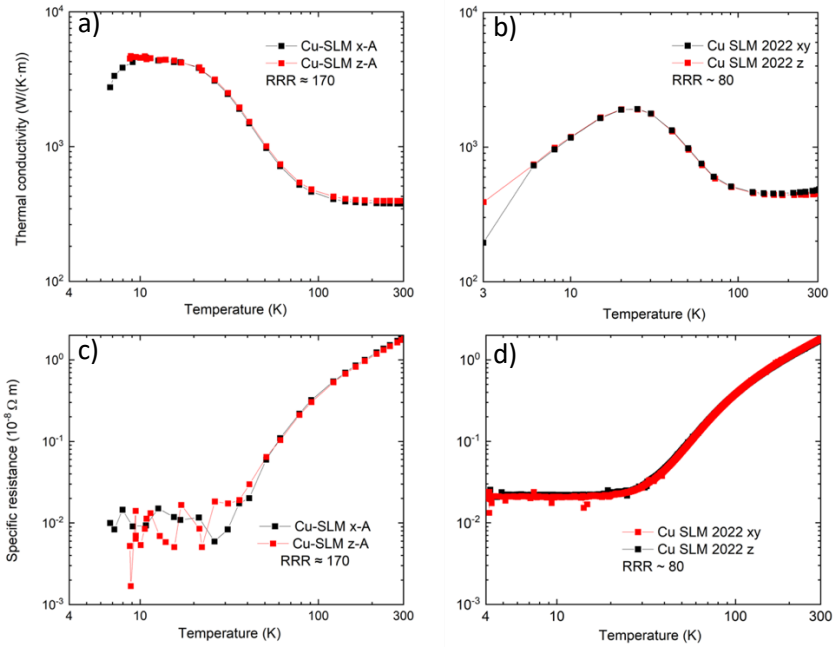

Figure 11. Comparison of the two different Cu SLM samples regarding transport measurement of thermal conductivity (a & b) and specific resistance (c & d). On the left side the results of the optimized process with *RRR*≈170 amd on the right-side the non-optimized *RRR*≈80.

Table 6. Vickers hardness tests at room temperature on Cu-SLM

Cu-SLM	*RRR* (273K/5K)	H_V (xy-dir)	H_V (z-dir)
Non-optimized	80 (+/- 4)	69.8 (+/- 1.9)	73.7 (+/-2.7)
optimized	170 (+/- 10)	48.9 (+/- 0.9)	53.1 (+/- 0.2)

4.6. Cu-Coldspray comparison

As mentioned above, the copper cube fabricated by the CS method has more relevant distortions compared to the SLM process. Therefore, a copper cube produced by the CS method was investigated in the same way as the copper produced by SLM. Figure 12 shows the result of the transport measurements. The *RRR* value is used to compare the electrical transport or resistivity measurement. As expected, the as-build condition results in the significant lower *RRR* of about 40, half of the as-build SLM, verifying the conclusion taken from the microstructure examination shown in Figure 3 and shown in detail in Figure 13. For the SLM the overall grain size is larger and no deformation twins of cracks as for CS are visible. Therefore, the less distorted copper SLM material exhibit higher conductivity also expressed by the *RRR* values. Accompanied with the lower *RRR* value of the copper CS material, the H_V is significantly higher, again with high values for indentation in z direction compared to the xy-direction.

Since the CS method is very attractive for additive manufacturing and a possible future multi-material composite, optimization to reduce distortion (e.g. grain size grow) was performed using different annealing temperatures. First material of the as-build copper CS material was annealed in argon atmosphere at 400°C for 2h. A second material block of the as-build copper CS material was annealed in argon at higher temperature of 650°C for 2h. Thermal and electrical transport measurements were performed and the *RRR* as well as the H_V was obtained. In Figure 12 the transport measurements experience a significant improvement of the *RRR* values of about 90 up to 132 for the 400°C and the 650°C treatment, respectively. The H_V (see Table 7) values drop accordingly with the increase of the *RRR*, due to the grain growth and reduction of the distortion within the copper CS material imposed by

the heat treatment. Comparing the copper SLM non-optimized to the copper CS 400°C annealed, similar results in conductivity and hardness are visible.

As the material properties scale in the same way as copper bulk with the *RRR* parameter [19, 20, 24], favorable thermo-physical properties can be adjusted by applying typical annealing treatments on the copper material [27, 28].

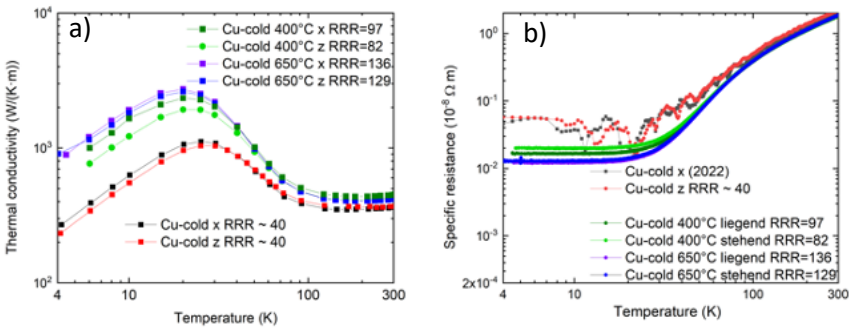

Figure 12. transport measurements of thermal conductivity (a) and specific resistance (b) of Cu coldspray as-build (*RRR*≈40) and after thermal heat treatment at 400°C (*RRR*≈90) and 650°C (*RRR*≈132) in z-direction and xy-direction.

Table 7. Vickers hardness tests at room temperature on Cu-coldspray

Cu-CS	*RRR* (273K/5K)	H_V (xy-dir)	H_V (z-dir)
Non-optimized	40 (+/- 3)	101.3 (+/- 1.1)	111.0 (+/- 4.0)
400°C / 2h	90 (+/- 8)	66.9 (+/- 1.4)	78.2 (+/- 0.6)
650°C / 2h	132 (+/- 4)	58.7 (+/- 0.4)	66.2 (+/- 2.1)

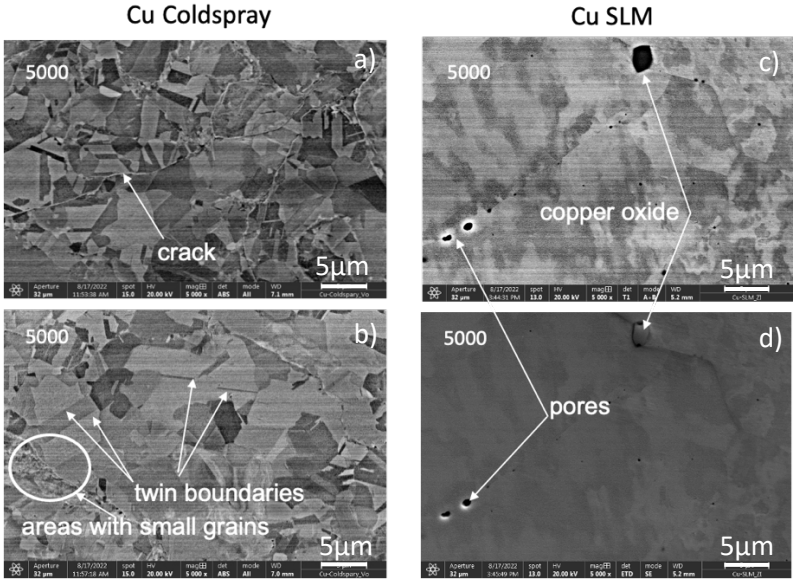

Figure 13. SEM-BSE images in z-direction of Cu-CS (a & b) showing cracks, twin boundaries and very small grain structure compared to Cu-SLM (c & d) with a significant low defect density.

5. FEM material database interface

In order to combine the simulation process of the hydrogen electrical propulsion system by a digital-twin with real world data, the material properties are assembled in a database file with spreadsheets. To incorporate the data into a FEM (*finite element method*) software such as COMSOL®, a python script was created to read the data and convert the information into a file readable for the FEM software as

three-dimensional tensor where appropriate. The material properties are included in the general material library of the system and can be chosen according to the required additive manufacturing process (CS, SLM, DED) and treatment condition (e.g. for copper by *RRR* value). With this a direct physical coupling in the calculations of the various components regarding mechanical or thermal behavior is possible. Interfaces for others FEM software are in preparation.

6. Summary and outlook

Due to the lack of comprehensive thermo-physical material data in the cryogenic regime of additively manufactured pure copper, Scalmalloy®, Ti-6Al-4V, and Inconel 718, measurements were conducted in a temperature range from about 4 K up to 300 K and above. The results are comparable to measurements of the related bulk material obtained from literature. By using appropriate annealing processes, as shown for copper CS, the thermo-physical properties can be adjusted for cryogenic applications.

Combining the electrical/thermal transport, thermal expansion, specific heat measurements with mechanical characterizations done by Fraunhofer Institute [9, 10] completes the detailed evaluation of the materials for the realization of relevant components [7, 8].

Further investigations are to be carried out on non-metallic materials like CFRP (carbon fiber reinforced plastics) [29, 30] and especially on interface CFRP-to-metal structures [5]. A promising development is seen in the application of DED for multi-material structures, where different alloys are combined to obtain a weld free transition. However, challenges such as different thermal expansion, surface adhesion of different metal combinations still need to be solved and will be addressed in upcoming projects.

An important issue is the reliability of the results obtained. As the variations in material composition as well as the manufacturing process become more complex, comparative references are crucial. Although excessive calibration is performed prior to measurement campaigns, there is always the question of the effects of the method and the calibration material. For this reason, a round robin test of European laboratories on thermal expansion was started to compare different methods, sample sizes and calibration materials in order to obtain a satisfactory answer from this measurement campaign and to provide quantitative reliable values for the uncertainty. In a next step, a round robin test for thermal conductivity will be organized.

7. References

[1] Blakey-Milner B, Gradl P, Snedden G, Brooks M, Pitot J, Lopez E, Leary M, Berto F and du Plessis A, 2021 *Materials & Design* **209** 110008

[2] Alvarez P, Satrústegui M, Elosegui I and Martinez-Iturralde M, 2022 *IEEE Access* **10** 10.1109/ACCESS.2022.3215692

[3] Weidermann C, Kloepzig M, Wilke M, Linde M and Rehme O, "Additive Manufacturing and hybrid materials in high power density machines for electric propulsion of vehicles" presented at *International Cryogenic Material Conference*, Honolulu, Hawaii, USA (2023) www.cec-icmc.org

[4] Filipenko M, Kühn L, Gleixner T, Thummet M, Lessmann M, Möller D, Böhm M, Schröter A, Häse K, Grundmann J, Wilke M, Frank M, van Hasselt P, Richter J, Herranz-Garcia M, Weidermann C, Spangolo A, Klöpzig M, Gröppel P and Moldenhauer S, 2020 *Supercond Sci Technol* **33**(5) 054002

[5] Pohl M, Spitzer S, Grothe R, Weidermann Ch and Gude M, "2022 *IOP Conf. Ser.: Mater. Sci. Eng.* **1226** 012077

[6] Pohl M, Weidermann C, Gude M, Modler N, Grothe R and Spitzer S,"New concept for cryogenic gaseous hydrogen-cooled lightweight electric engine", presented at *International Cryogenic Material Conference*, Honolulu, Hawaii, USA (2023) www.cec-icmc.org

[7] Vietze M and Weiland S, 2022 *International Journal of Hydrogen Energy* **47** 38793e38810

[8] Vietze M and Evrim C, "Development of additively manufactured cryogenic heat exchangers for hydrogen-electric aircraft propulsion" presented at *Cryogenic Engineering Conference*, Honolulu, Hawaii, USA (2023) www.cec-icmc.org

[9] Ebling F, Oesterlin H, Wackermann K, Primus D and Rehme O, 2022 *Proceedings of the Fourth International Conference on Metals & Hydrogen*, B02, ISBN 9789081794237
[10] Ebling F and Wackermann K, "Cryogenic material testing with gaseous hydrogen for hydrogen-electric aircraft propulsion" presented at *International Cryogenic Material Conference*, Honolulu, Hawaii, USA (2023) www.cec-icmc.org
[11] Rehme O and Weidermann C, "Additive Manufacturing of Cryogenic Materials", presented at *International Cryogenic Material Conference*, Honolulu, Hawaii, USA (2023) www.cec-icmc.org
[12] Bagrets N, Weiss E, Westenfelder S and Weiss K-P, 2012 *IEEE Trans Appl Supercond* **22**(3) 9501204
[13] Sas J, Weiss K-P and Bagrets N, 2015 *Acta Metallurgica Slovaca* **21**(4) 330-338
[14] Stautner W, Vanapalli, Weiss K-P, Chen R, Amm K, Budesheim E and Ricci J, 2017 *IOP Conference Series: Materials Science and Engineering* **278**(1) 012134
[15] Weiss K-P, Bagrets N, Lange C, Goldacker W and Wolgemuth J, 2015 *IOP Conference Series: Materials Science and Engineering* **102**(1) 012022
[16] Weiss K-P, Hetzler S, Kvackaj T, Bidulsky R, Actis Grande M and Manfredi D, 2022 *IOP Conf. Ser.: Mater. Sci. Eng.* **1241** 012047
[17] Bidulsky R, Bidulska J, Gobber FS, Kvackaj T, Petrousek P, Actis-Grande M, Weiss, K-P and Manfredi D, 2020 *Materials* **13** 3328
[18] Quantum-Design PPMS Measurement Options https://qdusa.com/products/ppms.html
[19] Bradley PE, Radebaugh R and Lewis MA, 2006 *Proceedings of ICMC '06 Twenty First International Cryogenic Engineering Conference and 9th Cryogenics*, 13–21
[20] Copper Development Association Inc. https://www.copper.org/resources/properties/cryogenic/
[21] Metallic Materials Properties Development and Standardization, 2023, Chapt.5, www.batelle.org
[22] Ridgeon FJ, Raine MJ, Halliday DP, Lakrimi M, Thomas A and Hampshire DP, 2017 *IEEE TransApplSupercon*, **27**(4) 4201205
[23] Draper SL, Lerch BA, Telesman J, Martin RE, Locci IE, Garg A and Ring AJ, 2016 *NASA/TM—2016-219136*
[24] Duthil P, 2013 *Proceedings of the CAS-CERN Accelerator School: Superconductivity for Accelerators*, Erice, Italy 24 April – 4 May 2013 CERN-2013-005
[25] Bolzoni L, Ruiz-Navas EM and Gordo E, 2013 *Materials and Design* **52** 888–895
[26] Lee SH, Kim SW and Kang KH, 2006 *International Journal of Thermophysics* **27**(1) 282-292
[27] Cho JH, Jin YM, Park DY, Kim HJ, Oh IK and Lee KA, 2011 *Met. Mater. Int.* **17**(1) 157-166
[28] Li, WY, LCJ and Liao H, 2006 *Journal of Thermal Spray Technology* **15** 206-211
[29] Hohe J, Schober M, Weiss K-P and Appel S, 2021 *CEAS Space Journal* **13** 145–153
[30] Hohe J, Schober M, Weiss K-P and Appel S, 2022 *Composites Science and Technology* **228** 109631

Acknowledgments
Supported by the Federal Ministry for Economic Affairs and Climate Action of the Federal Republic of Germany. Grant-No.: 20M1904D.